6th European Conference on Computational Mechanics (ECCM 6)
7th European Conference on Computational Fluid Dynamics (ECFD 7)
1115 June 2018, Glasgow, UK

ENERGY-MOMENTUM-ENTROPY CONSISTENT NUMERICAL METHODS FOR THERMOMECHANICAL SOLIDS BASED ON THE GENERIC FORMALISM

Mark Schiebl, Peter Betsch

Institute of Mechanics, Karlsruhe Institute of Technology, Germany
Otto-Ammann-Platz 9, 76131 Karlsruhe
{mark.schiebl,peter.betsch}@kit.edu, www.ifm.kit.edu

Key words: Thermomechanical Problems, Thermoelasticity, Structure-Preserving Numerical Methods

Abstract. We use the newly proposed GENERIC-based variational formulation for initial boundary value problems of finite strain thermoelasticity to design structure-preserving numerical methods. Therefore we first perform a discretization in space introducing a L_2 projection equation to keep the necessary test functions in the finite element space. Temporal discretization is then carried out using discrete derivatives to finally obtain Energy-Momentum-Entropy (EME) consistent numerical methods with enhanced numerical stability and robustness.

1 INTRODUCTION

The GENERIC (General Equation for the Non-Equilibrium Reversible-Irreversible Coupling) framework is a double-generator formalism for the thermodynamically consistent formulation of coupled problems in which the reversible and the irreversible contribution to the time evolution equation are additively split. For a comprehensive account on the GENERIC framework we refer to the book of Öttinger [1].
The extension of GENERIC framework to solid mechanics has been performed recently (see [2]-[4]). The great potential of the GENERIC framework has been recognized by Romero [5, 6] for the construction of structure-preserving numerical methods and termed this schemes thermodynamically consistent (TC) schemes (see also [7]-[11]). If the TC scheme is additionally capable to conserve momentum maps associated to symmetries of the underlying systems the resulting scheme may be also termed Energy-Momentum-Entropy (EME) scheme which can be viewed as the extensions to irreversible systems of earlier Energy-Momentum (EM) schemes for

reversible systems with symmetry such as large strains elastodynamics and flexible multibody dynamics. We refer to [12] for a comprehensive overview of previous developments. The limitations of the previously developed GENERIC-based numerical methods for thermomechanically coupled solids, namely (i) the restriction to the use of the entropy density as thermodynamical variable, and (ii) the restriction to isolated (or closed) systems, have been resolved in the companion contribution (see [15]). Full details of the proposed approach can be found in our recent work [13]. We therefore use this newly proposed generalized GENERIC-based variational formulation which (i) allows for the free choice of the thermodynamical variable among either the absolute temperature, the internal energy density or the entropy density and which (ii) takes boundary effects into account. This GENERIC-based variational formulation for large strain elastodynamics is then used as the basis for the construction of EME numerical methods as will be shown subsequently.

2 GENERIC-BASED VARIATIONAL FORMULATION FOR OPEN THERMO-ELASTO-DYNAMICAL SYSTEMS

We first consider a continuum body with material points $\mathbf{X} = X_i \mathbf{e}_i$ in the reference configuration $\mathcal{B} \subset \mathbb{R}^3$ (Fig. 1). Here and in the sequel the summation convention applies to repeated indices. Moreover, $\mathbf{e}_i$ denote the canonical base vectors in $\mathbb{R}^3$.

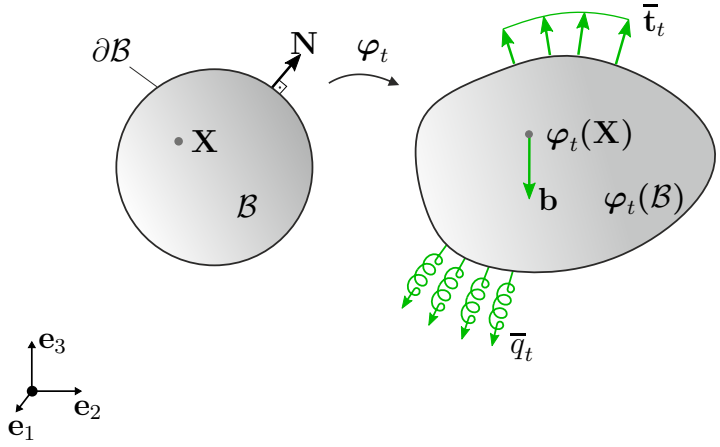

Figure 1: Reference configuration $\mathcal{B}$ with boundary $\partial\mathcal{B}$ and current configuration $\varphi_t(\mathcal{B})$ at time t. External tractions $\overline{\mathbf{t}}_t = \mathbf{P}_t\mathbf{N}$ act on the boundary of the current configuration. In addition to that, the heat flux across the current boundary is denoted by $\overline{q}_t = \mathbf{Q}_t \cdot \mathbf{N}$.

Within the Lagrangian description of continuum mechanics the deformed config-

uration of the body at time t is characterized by the deformation map $\boldsymbol{\varphi}_t : \mathcal{B} \mapsto \mathbb{R}^3$. The velocity of the material point $\mathbf{X} \in \mathcal{B}$ located at $\mathbf{x} = \boldsymbol{\varphi}_t(\mathbf{X})$ is given by $\mathbf{v}_t = \partial\boldsymbol{\varphi}_t/\partial t$. Alternatively we will often write $\mathbf{v}_t = \dot{\boldsymbol{\varphi}}_t$. The conjugate momentum density is defined by $\mathbf{p}_t = \rho\mathbf{v}_t$. The deformation gradient corresponds to the Jacobian of the deformation map, $\mathbf{F}_t = \partial\boldsymbol{\varphi}_t/\partial\mathbf{X}$. In what follows the partial derivative with respect to the material coordinates will be denoted by the nabla operator. Accordingly, the deformation gradient assumes the form

$$\mathbf{F}_t = \nabla\boldsymbol{\varphi}_t \tag{1}$$

A natural choice for the thermodynamic state variable is the absolute temperature $\theta_t : \mathcal{B} \mapsto \mathbb{R}_+$. Alternatively, the entropy density $\eta_t : \mathcal{B} \mapsto \mathbb{R}$ or the internal energy density $u_t : \mathcal{B} \mapsto \mathbb{R}$ could be chosen.
Before we can state the variational problem we need to deal with the initial boundary value problem (IBVP) pertaining to large strain thermoelastodynamics. For this we decompose the boundary $\mathcal{B}$ of the continuum into a displacement boundary $\partial_\varphi\mathcal{B}$, on which $\boldsymbol{\varphi}_t = \overline{\boldsymbol{\varphi}}_t$, and a traction boundary $\partial_\sigma\mathcal{B}$, on which $\mathbf{P}_t\mathbf{N} = \overline{\mathbf{t}}_t$, where $\overline{\boldsymbol{\varphi}}_t$ and $\overline{\mathbf{t}}_t$ are prescribed functions for $t \geq 0$. Moreover, $\partial_\varphi\mathcal{B} \cup \partial_\sigma\mathcal{B} = \partial\mathcal{B}$ and $\partial_\varphi\mathcal{B} \cap \partial_\sigma\mathcal{B} = \varnothing$. In this context we introduce the first Piola-Kirchhoff stress tensor

$$\mathbf{P}_t = \mathbf{P}'_t(\nabla\boldsymbol{\varphi}_t, \tau_t) = \partial_{\nabla\boldsymbol{\varphi}} u'(\nabla\boldsymbol{\varphi}_t, \tau_t) - \frac{\partial_\tau u'(\nabla\boldsymbol{\varphi}_t, \tau_t)}{\partial_\tau \eta'(\nabla\boldsymbol{\varphi}_t, \tau_t)} \partial_{\nabla\boldsymbol{\varphi}} \eta'(\nabla\boldsymbol{\varphi}_t, \tau_t) \tag{2}$$

whereas the absolute temperature is given via the important formula (see [1] and [3])

$$\theta'(\nabla\boldsymbol{\varphi}_t, \tau_t) = \frac{\partial_\tau u'(\nabla\boldsymbol{\varphi}_t, \tau_t)}{\partial_\tau \eta'(\nabla\boldsymbol{\varphi}_t, \tau_t)} \tag{3}$$

Similarly, for the thermal part we consider the subsets $\partial_\tau\mathcal{B}$ and $\partial_q\mathcal{B}$, with the properties $\partial_\tau\mathcal{B} \cup \partial_q\mathcal{B} = \partial\mathcal{B}$ and $\partial_\tau\mathcal{B} \cap \partial_q\mathcal{B} = \varnothing$. Here, the thermodynamic variable is prescribed on $\partial_\tau\mathcal{B}$, i.e. $\tau_t = \overline{\tau}_t$, whereas the heat flux is prescribed on $\partial_q\mathcal{B}$, i.e. $\mathbf{Q}_t \cdot \mathbf{N} = \overline{q}_t$.
Further, we introduce the material heat flux vector $\mathbf{Q}_t : \mathcal{B} \mapsto \mathbb{R}^3$ through $\mathbf{Q}_t = \mathbf{Q}'(\nabla\boldsymbol{\varphi}_t, \tau_t)$, where

$$\begin{aligned} \mathbf{Q}' &= (\theta')^2 \mathbf{K}_t \nabla \left(\frac{\partial_\tau \eta'}{\partial_\tau u'} \right) \\ &= -\mathbf{K}_t \nabla\theta' \end{aligned} \tag{4}$$

and where $\mathbf{K}_t = \mathbf{K}'_t$ is the positive semi-definite material conductivity tensor. We seek a formalism to determine the motion $\boldsymbol{\varphi}_t : \mathcal{B} \mapsto \mathbb{R}^3$, the linear momentum density $\mathbf{p}_t : \mathcal{B} \mapsto \mathbb{R}^3$ and the thermodynamic variable $\tau_t : \mathcal{B} \mapsto \mathbb{R}$ for $t \in (0, T]$ with initial conditions of the form $\boldsymbol{\varphi}_0 = \mathbf{X}$, $\mathbf{p}_0 = \rho\mathbf{V}_0$, and $\tau_0 = \tau^{\text{ini}}$ in $\mathcal{B}$. Here $\mathbf{V}_0$ is a prescribed

material velocity field and τ^{ini} is a prescribed field of the thermodynamic variable $\tau \in \{\theta, \eta, u\}$. We state the following GENERIC-based variational formulation for the present IBVP at hand

$$\begin{aligned} 0 &= \int_{\mathcal{B}} \mathbf{w}_{\varphi} \cdot \left(\dot{\boldsymbol{\varphi}}_t - \frac{1}{\rho} \mathbf{p}_t \right) \mathrm{d}V \\ 0 &= \int_{\mathcal{B}} \left(\mathbf{w}_{\mathrm{p}} \cdot (\dot{\mathbf{p}}_t - \mathbf{b}) + \mathbf{P}' : \nabla \mathbf{w}_{\mathrm{p}} \right) \mathrm{d}V - \int_{\partial_\sigma \mathcal{B}} \mathbf{w}_{\mathrm{p}} \cdot \overline{\mathbf{t}}_t \, \mathrm{d}A \\ 0 &= \int_{\mathcal{B}} \left(\mathrm{w}_\tau \dot{\tau}_t + \nabla (\frac{1}{\rho} \mathbf{p}_t) : \left(\frac{\mathrm{w}_\tau}{\partial_\tau \eta'} \partial_{\nabla \boldsymbol{\varphi}} \eta' \right) - \nabla \left(\frac{\mathrm{w}_\tau}{\partial_\tau u'} \right) \cdot \mathbf{Q}' \right) \mathrm{d}V + \int_{\partial_q \mathcal{B}} \frac{\mathrm{w}_\tau}{\partial_\tau u'} \overline{q}_t \, \mathrm{d}A \end{aligned} \tag{5}$$

and refer to [13, 15] for further details on the GENERIC-based variational formulation of large strain thermoelastodynamics where also important balance laws are directly deduced from it's variational form. Here, $\mathbf{w}_{\varphi}, \mathbf{w}_{\mathrm{p}} : \mathcal{B} \mapsto \mathbb{R}^3$ and $\mathrm{w}_\tau : \mathcal{B} \mapsto \mathbb{R}$ are test functions which have to satisfy the boundary conditions $\mathbf{w}_{\varphi} = \mathbf{0}$ and $\mathbf{w}_{\mathrm{p}} = \mathbf{0}$ on $\partial_{\varphi} \mathcal{B}$, and $\mathrm{w}_\tau = 0$ on $\partial_\tau \mathcal{B}$. These equations have to hold for all times $t \geq 0$ and for arbitrary test functions subject to the above mentioned boundary conditions.
Frame-indifferent arguments require that the functions of u' and η' can be expressed as

$$\begin{aligned} u'(\nabla \boldsymbol{\varphi}_t, \tau_t) &= u''(\mathbf{C}_t, \tau_t) \\ \eta'(\nabla \boldsymbol{\varphi}_t, \tau_t) &= \eta''(\mathbf{C}_t, \tau_t) \end{aligned} \tag{6}$$

where $\mathbf{C}_t = \mathbf{F}_t^{\mathrm{T}} \mathbf{F}_t$ is the right Cauchy-Green tensor written in terms of the deformation gradient $\mathbf{F}_t$. Taking (6) into account, we obtain

$$\begin{aligned} \partial_{\nabla \boldsymbol{\varphi}} u' &= 2 \mathbf{F}_t \partial_{\mathbf{C}} u''(\mathbf{C}, \tau) \\ \partial_{\nabla \boldsymbol{\varphi}} \eta' &= 2 \mathbf{F}_t \partial_{\mathbf{C}} \eta''(\mathbf{C}, \tau) \end{aligned} \tag{7}$$

together with

$$\begin{aligned} \partial_\tau u' &= \partial_\tau u''(\mathbf{C}, \tau) \\ \partial_\tau \eta' &= \partial_\tau \eta''(\mathbf{C}, \tau) \end{aligned} \tag{8}$$

3 STRUCTURE-PRESERVING SCHEMES

3.1 Discretization in space

We first perform the discretization in space of the variational formulation. Therefore we apply standard isoparametric finite elements based on finite dimensional approximations of the state variables at time t, given by

$$\boldsymbol{\varphi}_{\mathrm{t}}^{\mathrm{h}}(\mathbf{X}) = \sum_{a=1}^{n_{node}} N^a(\mathbf{X}) \, \boldsymbol{\varphi}_a(t) \,, \qquad \mathbf{p}_{\mathrm{t}}^{\mathrm{h}}(\mathbf{X}) = \sum_{a=1}^{n_{node}} N^a(\mathbf{X}) \, \mathbf{p}_a(t) \tag{9}$$

and

$$\tau_{\mathrm{t}}^{\mathrm{h}}(\mathbf{X}) = \sum_{a=1}^{n_{node}} N^a(\mathbf{X})\, \tau_a(t) \tag{10}$$

Here, $N^a : \mathcal{B} \to \mathbb{R}$ denote the nodal shape functions and $\boldsymbol{\varphi}_a(t), \mathbf{p}_a(t) \in \mathbb{R}^3$, $\tau_a(t) \in \mathbb{R}$ are the respective nodal values at time t. Moreover, n_{node} denotes the total number of nodes in the finite element mesh. The standard (Bubnov) Galerkin approach relies on analogous approximations for the test functions in the variational equations (5), $\mathbf{w}_\varphi, \mathbf{w}_{\mathrm{p}}$ and w_τ, denoted by $\mathbf{w}_\varphi^{\mathrm{h}}, \mathbf{w}_{\mathrm{p}}^{\mathrm{h}}$ and w_τ^{h}.
The semi-discrete problem then takes the following form

$$\begin{aligned}
0 &= \int_{\mathcal{B}} \mathbf{w}_\varphi^{\mathrm{h}} \cdot \left(\dot{\boldsymbol{\varphi}}_t^{\mathrm{h}} - \frac{1}{\rho} \mathbf{p}_t^{\mathrm{h}} \right) \mathrm{d}V \\
0 &= \int_{\mathcal{B}} \left(\mathbf{w}_{\mathrm{p}}^{\mathrm{h}} \cdot \left(\dot{\mathbf{p}}_t^{\mathrm{h}} - \mathbf{b}^{\mathrm{h}} \right) + \mathbf{P}^{\mathrm{h}'} : \nabla \mathbf{w}_{\mathrm{p}}^{\mathrm{h}} \right) \mathrm{d}V - \int_{\partial_\sigma \mathcal{B}} \mathbf{w}_{\mathrm{p}}^{\mathrm{h}} \cdot \overline{\mathbf{t}}_t^{\mathrm{h}} \, \mathrm{d}A \\
0 &= \int_{\mathcal{B}} \left(\mathrm{w}_\tau^{\mathrm{h}} \dot{\tau}_t^{\mathrm{h}} + \nabla(\frac{1}{\rho} \mathbf{p}_t^{\mathrm{h}}) : \left(\frac{\mathrm{w}_\tau^{\mathrm{h}}}{\partial_\tau \eta^{\mathrm{h}''}} \partial_\nabla \boldsymbol{\varphi} \eta^{\mathrm{h}'} \right) - \nabla \left(\frac{\mathrm{w}_\tau^{\mathrm{h}}}{\partial_\tau u^{\mathrm{h}''}} \right) \cdot \mathbf{Q}^{\mathrm{h}''} \right) \mathrm{d}V + \int_{\partial_q \mathcal{B}} \frac{\mathrm{w}_\tau^{\mathrm{h}}}{\partial_\tau u^{\mathrm{h}''}} \overline{q}_t^{\mathrm{h}} \, \mathrm{d}A
\end{aligned} \tag{11}$$

Following the procedure in [13, 15] for the verification of the important balance laws, namely the balance of the total angular momentum, the balance of energy and the balance of entropy, specific choices for the test functions in (11) have to be made. Depending on the specific choice for the thermodynamic variable, these test functions may not belong to the finite element space. Therefore a simple modification (see [6, 9] for more details) is introduced to maintain the satisfaction of the balance laws in the semi-discrete setting. Whenever the semi-discrete approximations $w_\tau^h = \partial_\tau \square^{\mathrm{h}}$, where $\square \in \{u'', \eta''\}$, are not in the finite element space, a L_2 projection of the specific quantity onto the finite element space need to be performed, where all the previous approximation $\partial_\tau \square^{\mathrm{h}}$ need to be replaced with it's projected counterpart. The L_2 projection equation is of the following form

$$0 = \int_{\mathcal{B}} w_{\mathrm{pr}}^{\mathrm{h}} (\partial_\tau \square^{\mathrm{h}} - \partial_\tau^{\mathrm{pr}} \square^{\mathrm{h}}) \, \mathrm{d}V, \quad \text{where} \quad \partial_\tau^{\mathrm{pr}} \square^{\mathrm{h}} = \sum_{a=1}^{n_{node}} N^a(\mathbf{X})\, \partial_\tau \, \square_a \, (t) \tag{12}$$

and where $w_{\mathrm{pr}}^{\mathrm{h}} : \mathcal{B} \mapsto \mathbb{R}$ is a discrete test function.

Remark 1. *For the formulations in the inner energy and the entropy density only one projection need to be carried out whereas for the formulation in the absolute temperature two projections are in general necessary for the verification of the important balance laws in the semi-discrete settings (see Table 1 for more details). If the specific heat capacity is chosen to be constant (see i.e. (21)) the formulation in the absolute temperature reduces to one projection equation as well.*

The resulting scheme then takes the following form

$$
\begin{aligned}
0 &= \int_{\mathcal{B}} \mathbf{w}_{\varphi}^{\mathrm{h}} \cdot \left(\dot{\boldsymbol{\varphi}}_t^{\mathrm{h}} - \frac{1}{\rho} \mathbf{p}_t^{\mathrm{h}} \right) \mathrm{d}V \\
0 &= \int_{\mathcal{B}} \left(\mathbf{w}_{\mathrm{p}}^{\mathrm{h}} \cdot \left(\dot{\mathbf{p}}_t^{\mathrm{h}} - \mathbf{b}^{\mathrm{h}} \right) + \mathbf{P}^{\mathrm{h}'} : \nabla \mathbf{w}_{\mathrm{p}}^{\mathrm{h}} \right) \mathrm{d}V - \int_{\partial_\sigma \mathcal{B}} \mathbf{w}_{\mathrm{p}}^{\mathrm{h}} \cdot \overline{\mathbf{t}}_t^{\mathrm{h}} \, \mathrm{d}A \\
0 &= \int_{\mathcal{B}} \left(\mathrm{w}_\tau^{\mathrm{h}} \dot{\tau}_t^{\mathrm{h}} + \nabla \left(\frac{1}{\rho} \mathbf{p}_t^{\mathrm{h}} \right) : \left(\frac{\mathrm{w}_\tau^{\mathrm{h}}}{\partial_\tau^{\mathrm{pr}} \eta_{\mathrm{algo}}^{\mathrm{h}''}} \partial_\nabla \boldsymbol{\varphi} \eta^{\mathrm{h}'} \right) - \nabla \left(\frac{\mathrm{w}_\tau^{\mathrm{h}}}{\partial_\tau^{\mathrm{pr}} u_{\mathrm{algo}}^{\mathrm{h}''}} \right) \cdot \mathbf{Q}^{\star \mathrm{h}''} \right) \mathrm{d}V \\
&\quad + \int_{\partial_q \mathcal{B}} \frac{\mathrm{w}_\tau^{\mathrm{h}}}{\partial_\tau^{\mathrm{pr}} u_{\mathrm{algo}}^{\mathrm{h}''}} \overline{q}_t^{\mathrm{h}} \, \mathrm{d}A \\
0 &= \int_{\mathcal{B}} w_{\mathrm{pr}}^{\mathrm{h}} \left(\partial_\tau \square^{\mathrm{h}''} - \partial_\tau^{\mathrm{pr}} \square^{\mathrm{h}''} \right) \mathrm{d}V
\end{aligned}
\tag{13}
$$

where

$$
\begin{aligned}
\mathbf{P}^{\mathrm{h}'} &= 2 \mathbf{F}_t^{\mathrm{h}} \left(\partial_{\mathbf{C}} u^{\mathrm{h}''} - \theta^{\star \mathrm{h}''} \partial_{\mathbf{C}} \eta^{\mathrm{h}''} \right) \\
\partial_\nabla \boldsymbol{\varphi} \eta^{\mathrm{h}'} &= 2 \mathbf{F}_t^{\mathrm{h}} \partial_{\mathbf{C}} \eta^{\mathrm{h}''}
\end{aligned}
\tag{14}
$$

It can be shown, that (13) preserves all key balance laws in the semi-discrete setting. The associated evaluation of the absolute temperature $\theta^{\star \mathrm{h}''}$, of the material heat flux vector $\mathbf{Q}^{\star \mathrm{h}''}$ and of the quantities $\partial^{\mathrm{pr}} \square_{\mathrm{algo}}^{\mathrm{h}''}$ can be found in Table 1, where for the semi-discrete case all time-discrete quantities have to be replaced with the corresponding time-continuous quantity.

3.2 Discretization in time

Finally we perform the discretization in time of the semi-discrete variational formulation eq. (13). To this end we focus on a representative time interval $[t_{\mathrm{n}}, t_{\mathrm{n+1}}]$ with corresponding time-step size $\Delta t = t_{\mathrm{n+1}} - t_{\mathrm{n}}$. The discrete approximations at times t_{n} and $t_{\mathrm{n+1}}$ of the continuous variable $(\bullet)_{\mathrm{t}}$ will be denoted by $(\bullet)_{\mathrm{n}}$ and $(\bullet)_{\mathrm{n+1}}$, respectively. Moreover, the approximation of any state variable $(\bullet)_{\mathrm{t}}$ at mid-point time $t_{\mathrm{n+\frac{1}{2}}} = \frac{1}{2}(t_{\mathrm{n}} + t_{\mathrm{n+1}})$ is given by $(\bullet)_{\mathrm{n+\frac{1}{2}}} = \frac{1}{2}\big((\bullet)_{\mathrm{n}} + (\bullet)_{\mathrm{n+1}}\big)$. Assume that the state variables $\boldsymbol{\varphi}_{\mathrm{n}}, \mathbf{p}_{\mathrm{n}} : \mathcal{B} \mapsto \mathbb{R}^3$ and $\tau_{\mathrm{n}} : \mathcal{B} \mapsto \mathbb{R}$, $\tau_{\mathrm{n}} \in \{\theta_{\mathrm{n}}, \eta_{\mathrm{n}}, u_{\mathrm{n}}\}$ are given.
We aim at the determination of the corresponding state variables $(\boldsymbol{\varphi}_{\mathrm{n+1}}, \mathbf{p}_{\mathrm{n+1}}, \tau_{\mathrm{n+1}})$. In this connection we make use of the notion of a discrete derivative in the sense of [16], where $\mathbf{P}_{\mathrm{algo}}^{\mathrm{h}'}$ is the algorithmic first Piola-Kirchhoff stress tensor and $\theta_{\mathrm{algo}}^{\star \mathrm{h}''}$ is the algorithmic absolute temperature. The evaluation of the algorithmic absolute temperature and of the material heat flux vector $\mathbf{Q}_{\mathrm{algo}}^{\star \mathrm{h}''}$ can be found in Table 1.

$$
\begin{aligned}
\mathbf{P}_{\mathrm{algo}}^{\mathrm{h}'} &= 2 \mathbf{F}_{\mathrm{n+\frac{1}{2}}}^{\mathrm{h}} \left(\bar{\mathrm{D}}_{\mathbf{C}} u^{\mathrm{h}''} - \theta_{\mathrm{algo}}^{\star \mathrm{h}''} \bar{\mathrm{D}}_{\mathbf{C}} \eta^{\mathrm{h}''} \right) \\
\partial_{\mathbf{F}} \eta_{\mathrm{algo}}^{\mathrm{h}'} &= 2 \mathbf{F}_{\mathrm{n+\frac{1}{2}}}^{\mathrm{h}} \bar{\mathrm{D}}_{\mathbf{C}} \eta^{\mathrm{h}''}
\end{aligned}
\tag{15}
$$

Accordingly, a discrete version of (5) is given by

$$
\begin{aligned}
0 &= \int_{\mathcal{B}} \mathbf{w}^{\mathrm{h}}_{\varphi} \cdot \left(\frac{\boldsymbol{\varphi}^{\mathrm{h}}_{\mathrm{n}+1} - \boldsymbol{\varphi}^{\mathrm{h}}_{\mathrm{n}}}{\Delta t} - \frac{1}{\rho} \mathbf{p}^{\mathrm{h}}_{\mathrm{n}+\frac{1}{2}} \right) \mathrm{d}V \\
0 &= \int_{\mathcal{B}} \left(\mathbf{w}^{\mathrm{h}}_{\mathrm{p}} \cdot \frac{\mathbf{p}^{\mathrm{h}}_{\mathrm{n}+1} - \mathbf{p}^{\mathrm{h}}_{\mathrm{n}}}{\Delta t} - \mathbf{w}^{\mathrm{h}}_{\mathrm{p}} \cdot \mathbf{b} + \nabla \mathbf{w}^{\mathrm{h}}_{\mathrm{p}} : \mathbf{P}^{\mathrm{h}'}_{\mathrm{algo}} \right) \mathrm{d}V - \int_{\partial_\sigma \mathcal{B}} \mathbf{w}^{\mathrm{h}}_{\mathrm{p}} \cdot \overline{\mathbf{t}}^{\mathrm{h}}_{\mathrm{n}+\frac{1}{2}} \, \mathrm{d}A \\
0 &= \int_{\mathcal{B}} \mathrm{w}^{\mathrm{h}}_{\tau} \left(\frac{\tau^{\mathrm{h}}_{\mathrm{n}+1} - \tau^{\mathrm{h}}_{\mathrm{n}}}{\Delta t} + \nabla \left(\frac{1}{\rho} \mathbf{p}^{\mathrm{h}}_{\mathrm{n}+\frac{1}{2}} \right) : \left(\frac{\partial_{\mathbf{F}} \eta^{\mathrm{h}'}_{\mathrm{algo}}}{\partial^{\mathrm{pr}}_{\tau} \eta^{\mathrm{h}''}_{\mathrm{algo}}} \right) \right) \mathrm{d}V \\
&\quad - \int_{\mathcal{B}} \nabla \left(\frac{\mathrm{w}^{\mathrm{h}}_{\tau}}{\partial^{\mathrm{pr}}_{\tau} u^{\mathrm{h}''}_{\mathrm{algo}}} \right) \cdot \mathbf{Q}^{\star \mathrm{h}''}_{\mathrm{algo}} \, \mathrm{d}V + \int_{\partial_q \mathcal{B}} \frac{\mathrm{w}^{\mathrm{h}}_{\tau}}{\partial^{\mathrm{pr}}_{\tau} u^{\mathrm{h}''}_{\mathrm{algo}}} \overline{q}^{\mathrm{h}}_{\mathrm{n}+\frac{1}{2}} \, \mathrm{d}A \\
0 &= \int_{\mathcal{B}} w^{\mathrm{h}}_{\mathrm{pr}} (\bar{\mathrm{D}}_{\tau} \square^{\mathrm{h}''} - \partial^{\mathrm{pr}}_{\tau} \square^{\mathrm{h}''}) \, \mathrm{d}V
\end{aligned}
\tag{16}
$$

To specify the specific discrete derivatives, $\bar{\mathrm{D}}_{\mathbf{C}} \square^{\mathrm{h}}$ and $\bar{\mathrm{D}}_{\tau} \square^{\mathrm{h}}$, we first collect the arguments of the density functions in the following vector

$$
\boldsymbol{\pi} = (\mathbf{C}, \tau) = (\pi^1, \pi^2) \tag{17}
$$

Using this notation we introduce partitioned discrete derivatives $\bar{\mathrm{D}}_{\pi^1} \square^{\mathrm{h}} = \bar{\mathrm{D}}_{\mathbf{C}} \square^{\mathrm{h}}$ and $\bar{\mathrm{D}}_{\pi^2} \square^{\mathrm{h}} = \bar{\mathrm{D}}_{\tau} \square^{\mathrm{h}}$ in the sense of [16] by

$$
\begin{aligned}
\bar{\mathrm{D}}_{\pi^i} \square^{\mathrm{h}} &= \frac{1}{2} (\bar{\mathrm{D}}_{\pi^i} \square^{\mathrm{h}}_{\mathrm{n}+1,\mathrm{n}} + \bar{\mathrm{D}}_{\pi^i} \square^{\mathrm{h}}_{\mathrm{n},\mathrm{n}+1}), \quad i \in Y = \{1, 2\} \\
\bar{\mathrm{D}}_{\pi^i_{\mathrm{n}+1,\mathrm{n}}} \square^{\mathrm{h}} &= \bar{\mathrm{D}}_{\pi^i} \square^{\mathrm{h}} \left(\pi^i_{n+1}, \pi^i_{\mathrm{n}} \right)\big|_{\pi^j_{n+1}, \pi^k_{\mathrm{n}}}, \quad \forall j \in Y : j < i, \, k \in Y : k > i \\
\bar{\mathrm{D}}_{\pi^i_{\mathrm{n},\mathrm{n}+1}} \square^{\mathrm{h}} &= \bar{\mathrm{D}}_{\pi^i} \square^{\mathrm{h}} \left(\pi^i_{\mathrm{n}}, \pi^i_{\mathrm{n}+1} \right)\big|_{\pi^j_{\mathrm{n}}, \pi^k_{\mathrm{n}+1}}, \quad \forall j \in Y : j < i, \, k \in Y : k > i
\end{aligned}
\tag{18}
$$

where the discrete operators $\bar{\mathrm{D}}_{\pi^i} \square^{\mathrm{h}} \left(\pi^i_{\mathrm{n}+1}, \pi^i_{\mathrm{n}} \right)\big|_{\pi^j_{\mathrm{n}+1}, \pi^k_{\mathrm{n}}}$ and $\bar{\mathrm{D}}_{\pi^i} \square^{\mathrm{h}} \left(\pi^i_{\mathrm{n}}, \pi^i_{\mathrm{n}+1} \right)\big|_{\pi^j_{\mathrm{n}}, \pi^k_{\mathrm{n}+1}}$ are defined as

$$
\begin{aligned}
\bar{\mathrm{D}}_{\pi^i} \square^{\mathrm{h}} \big|_{\pi^j_{\mathrm{n}+1}, \pi^k_{\mathrm{n}}} &= \partial_{\pi^i} \square^{\mathrm{h}} \left(\pi^i_{\mathrm{n}+\frac{1}{2}} \right)\big|_{\pi^j_{\mathrm{n}+1}, \pi^k_{\mathrm{n}}} \\
&\quad + \frac{\square^{\mathrm{h}}(\pi^i_{\mathrm{n}+1})\big|_{\pi^j_{\mathrm{n}+1}, \pi^k_{\mathrm{n}}} - \square^{\mathrm{h}}(\pi^i_{\mathrm{n}})\big|_{\pi^j_{\mathrm{n}+1}, \pi^k_{\mathrm{n}}} - \langle \partial_{\pi^i} \square^{\mathrm{h}} \left(\pi^i_{\mathrm{n}+\frac{1}{2}} \right)\big|_{\pi^j_{\mathrm{n}+1}, \pi^k_{\mathrm{n}}}, \Delta \pi^{i,\mathrm{h}} \rangle}{||\Delta \pi^{i,\mathrm{h}}||^2} \Delta \pi^{i,\mathrm{h}} \\
\bar{\mathrm{D}}_{\pi^i} \square^{\mathrm{h}} \big|_{\pi^j_{\mathrm{n}}, \pi^k_{\mathrm{n}+1}} &= \partial_{\pi^i} \square^{\mathrm{h}} \left(\pi^i_{\mathrm{n}+\frac{1}{2}} \right)\big|_{\pi^j_{\mathrm{n}}, \pi^k_{\mathrm{n}+1}} \\
&\quad + \frac{\square^{\mathrm{h}}(\pi^i_{\mathrm{n}+1})\big|_{\pi^j_{\mathrm{n}}, \pi^k_{\mathrm{n}+1}} - \square^{\mathrm{h}}(\pi^i_{\mathrm{n}})\big|_{\pi^j_{\mathrm{n}}, \pi^k_{\mathrm{n}+1}} - \langle \partial_{\pi^i} \square^{\mathrm{h}} \left(\pi^i_{\mathrm{n}+\frac{1}{2}} \right)\big|_{\pi^j_{\mathrm{n}}, \pi^k_{\mathrm{n}+1}}, \Delta \pi^{i,\mathrm{h}} \rangle}{||\Delta \pi^{i,\mathrm{h}}||^2} \Delta \pi^{i,\mathrm{h}}
\end{aligned}
\tag{19}
$$

Hereby $\langle .,. \rangle$ denotes the inner product and $\bar{\mathrm{D}}_{\pi^i}\square^{\mathrm{h}}$ the discrete gradient of $\square^{\mathrm{h}}$ with respect to π^i. It can be shown that eq. (16) preserves all key balance laws in the discrete setting and therefore represents a structure-preserving numerical method with enhanced numerical stability and robustness compared to classical methods (see [13] for GENERIC-based midpoint schemes).

Table 1: Resulting algorithmic absolute temperature and algorithmic material heat flux vector depending on the specific choices for τ

τ	$\partial_\tau u^{\mathrm{h}''}_{\mathrm{algo}}$	$\partial_\tau \eta^{\mathrm{h}''}_{\mathrm{algo}}$	$\theta^{\star\mathrm{h}''}_{\mathrm{algo}}$	$\mathbf{Q}^{\star\mathrm{h}''}_{\mathrm{algo}}$
η	$\partial^{\mathrm{pr}}_\eta \widetilde{u}^{\mathrm{h}}$	1	$\partial^{\mathrm{pr}}_\eta \widetilde{u}^{\mathrm{h}}$	$-\widetilde{\mathbf{K}}^{\mathrm{h}}_{\mathrm{n}+\frac{1}{2}} \nabla \widetilde{\theta}^{\star\mathrm{h}}_{\mathrm{algo}}$
θ	$\partial^{\mathrm{pr}}_\theta \bar{u}^{\mathrm{h}}$	$\partial^{\mathrm{pr}}_\theta \bar{\eta}^{\mathrm{h}}$	$\partial^{\mathrm{pr}}_\theta \bar{u}^{\mathrm{h}} [\partial^{\mathrm{pr}}_\theta \bar{\eta}^{\mathrm{h}}]^{-1}$	$-\bar{\mathbf{K}}^{\mathrm{h}}_{\mathrm{n}+\frac{1}{2}} \nabla \bar{\theta}^{\star\mathrm{h}}_{\mathrm{algo}}$
u	1	$\partial^{\mathrm{pr}}_u \widehat{\eta}^{\mathrm{h}}$	$[\partial^{\mathrm{pr}}_u \widehat{\eta}^{\mathrm{h}}]^{-1}$	$-\widehat{\mathbf{K}}^{\mathrm{h}}_{\mathrm{n}+\frac{1}{2}} \nabla \widehat{\theta}^{\star\mathrm{h}}_{\mathrm{algo}}$

4 MATERIAL MODEL

The Helmholtz free energy density that will be used in Section 5 is given by

$$\overline{\psi}(\nabla\boldsymbol{\varphi}, \theta) = \psi_1(\nabla\boldsymbol{\varphi}) + \psi_2(\theta) - (\theta - \theta_0)\psi_3(J) \tag{20}$$

where

$$\begin{aligned} \psi_1(\nabla\boldsymbol{\varphi}) &= \frac{\mu}{2}\left(\nabla\boldsymbol{\varphi} : \nabla\boldsymbol{\varphi} - 3 - 2\ln J - \frac{2}{3}(J-1)^2\right) + W_{\mathrm{vol}}(J) \\ \psi_2(\theta) &= c\,(\theta - \theta_0 - \theta \log(\theta/\theta_0)) \\ \psi_3(J) &= 3\beta W'_{\mathrm{vol}}(J) \\ W_{\mathrm{vol}}(J) &= \frac{\lambda + \frac{2}{3}\mu}{4}\left((\ln J)^2 + (J-1)^2\right) \end{aligned} \tag{21}$$

Here, $J = \det \nabla\boldsymbol{\varphi}$ is the determinant of the deformation gradient and μ, λ are prescribed parameters, $c > 0$ is the specific heat capacity at constant deformation, β is the coefficient of thermal expansion, and θ_0 is the reference temperature. Concerning the constitutive equation (4) for the material heat flux vector, we assume thermally isotropic material, with material conductivity tensor given by

$$\mathbf{K}_t = kJ\mathbf{C}^{-1} \tag{22}$$

5 NUMERICAL EXAMPLE

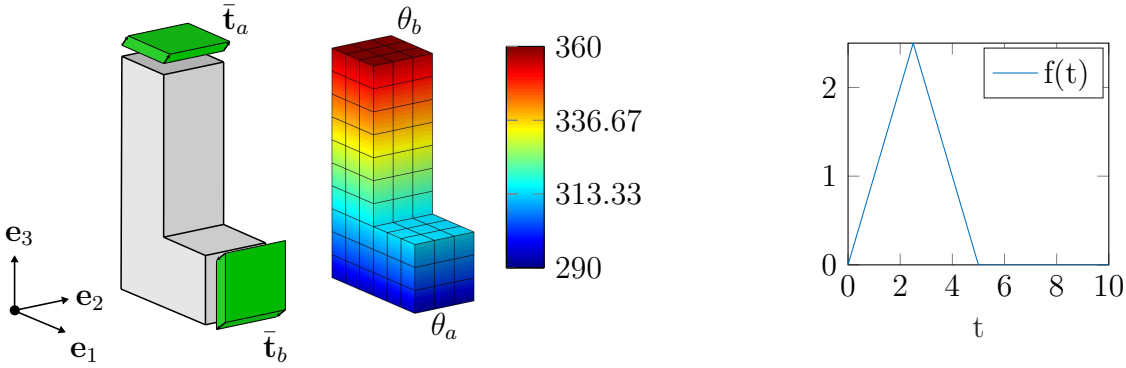

Figure 2: L-shaped block: Mechanical boundary conditions (left), discretised block with initial temperature distribution (middle), and load function over time (right)

The numerical example deals with the L-shaped block depicted in Fig. 2. The spatial discretization of the block relies on 117 tri-linear finite elements leading to 224 nodes. The initial temperature field is varying linearly over the height (x_3 direction) of the block. In particular, at $x_3 = 0$, the initial temperature is prescribed as θ_a, while at $x_3 = h$, the temperature is prescribed as θ_b. The whole block is assumed to be thermally insulated ($\overline{q}_t = 0$ on $\partial_q\mathcal{B} = \partial\mathcal{B}$). Starting at rest, Piola traction vectors $\bar{\mathbf{t}}_a$ and $\bar{\mathbf{t}}_b$ are acting on two parts of the boundary surface of the block (Fig. 2). The external loads are applied in the form of a hat function over time. In particular, the traction vectors are given by

$$\bar{\mathbf{t}}_a = -\bar{\mathbf{t}}_b = f(t)\begin{pmatrix}256/9\\512/9\\768/9\end{pmatrix}\text{Pa}, \quad f(t) = \begin{cases} t & \text{for} \quad 0\text{s} \le t \le 2.5\text{s} \\ 5-t & \text{for} \quad 2.5\text{s} \le t \le 5\text{s} \\ 0 & \text{for} \quad t > 5\text{s}. \end{cases} \tag{23}$$

Table 2 provides a summary of the data used in the simulations. No Dirichlet boundary conditions are applied. The Piola traction vectors introduce energy into the system, whereas after loading phase the total energy must be a conserved quantity. This simulation was investigated previously with the classical midpoint rule leading to numerical instabilities for larger time step sizes (see [13]). To emphasize the numerical stability and robustness of the $(\text{EME})_\tau$ integrators we chose the largest time step size in [13] which led to early instabilities and finally to a failure of the iterative (Newton-Raphson) solution procedure.

Table 2: L-shaped block: Data used in the simulations

Material parameters	μ	997.5	Pa
	λ		Pa
Specific heat capacity	c	100	$\mathrm{JK^{-1}m^{-3}}$
Coupling coefficient	β	$2.233 \cdot 10^{-4}$	$\mathrm{JK^{-1}}$
Thermal conductivity	k	10	$\mathrm{WK^{-1}m^{-1}}$
Ref. temperature	θ_0	293.15	K
Mass density	ρ	100	$\mathrm{kgm^{-3}}$
Initial temperature	θ_a	290	K
	θ_b	350	K
Geometry	h	10	m
	b	3	m
Newton tolerance	ε	10^{-8}	-
Simulation duration	T	250	s
Time step	Δt	0.4	s

Geometry of L-shape

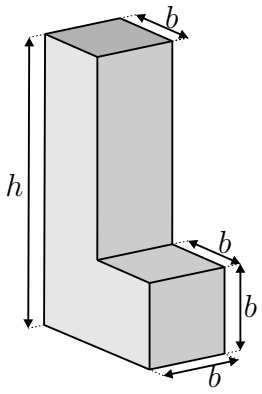

As expected, all $(\mathrm{EME})_\tau$ schemes correctly reproduce the first law of thermodynamics with energy conservation up to numerical precision after loading phase (up to numerical round-off), see Fig. 3 and 4. Further the total entropy ought to be a non-decreasing function of time since no entropy flux over the boundary is present during the simulation time which is correctly reproduced by all $(\mathrm{EME})_\tau$ schemes which can be observed in Fig 5 and 6.

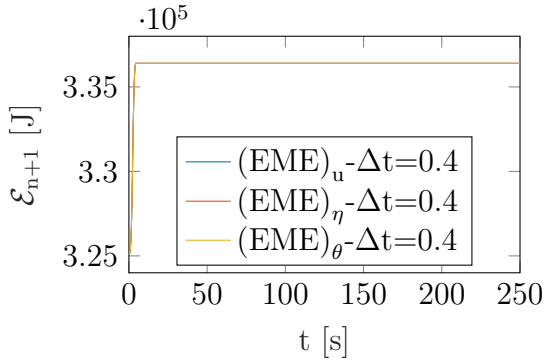

Figure 3: Total energy, $(\mathrm{EME})_\tau$ schemes

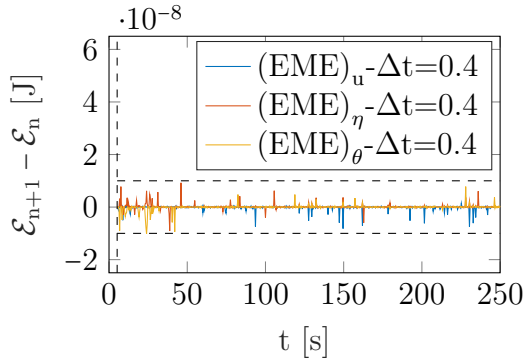

Figure 4: Discrete energy difference, $(\mathrm{EME})_\tau$ schemes

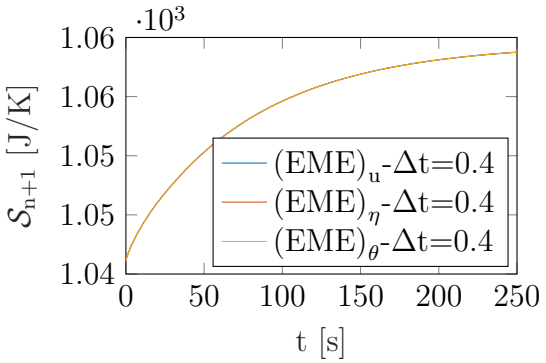

Figure 5: Total entropy, $(\mathrm{EME})_\tau$ schemes

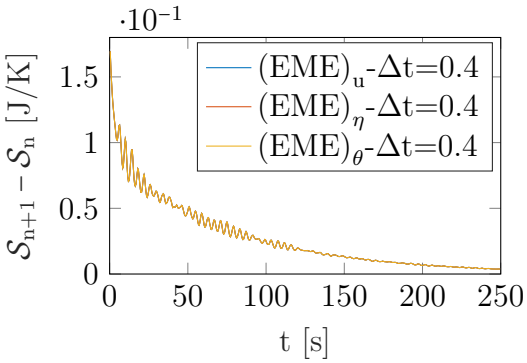

Figure 6: Discrete entropy difference, $(\mathrm{EME})_\tau$ schemes

ACKNOWLEDGMENT

Support for this research was provided by the Deutsche Forschungsgemeinschaft (DFG) under Grant BE 2285/13-1. This support is gratefully acknowledged.

REFERENCES

[1] H.C. Öttinger. *Beyond Equilibrium Thermodynamics*. John Wiley & Sons, 2005.

[2] M. Hütter and B. Svendsen. On the formulation of continuum thermodynamic models for solids as general equations for non-equilibrium reversible-irreversible coupling. *J. Elast.*, 104(1-2):357–368, 2011.

[3] A. Mielke. Formulation of thermoelastic dissipative material behavior using GENERIC. *Continuum Mech. Thermodyn.*, 23(3):233–256, 2011.

[4] M. Hütter and B. Svendsen. Thermodynamic model formulation for viscoplastic solids as general equations for non-equilibrium reversible-irreversible coupling. *Continuum Mech. Thermodyn.*, 24(3):211–227, 2012.

[5] I. Romero. Thermodynamically consistent time-stepping algorithms for non-linear thermomechanical systems. *Int. J. Numer. Meth. Engng*, 79(6):706–732, 2009.

[6] I. Romero. Algorithms for coupled problems that preserve symmetries and the laws of thermodynamics: Part I: Monolithic integrators and their application to finite strain thermoelasticity. *Comput. Methods Appl. Mech. Engrg.*, 199(25-28):1841–1858, 2010.

[7] M. Krüger, M. Groß, and P. Betsch. A comparison of structure-preserving integrators for discrete thermoelastic systems. *Computational Mechanics*, 47(6):701–722, 2011.

[8] S. Conde Martín, P. Betsch, and J.C. García Orden. A temperature-based thermodynamically consistent integration scheme for discrete thermo-elastodynamics. *Commun. Nonlinear Sci. Numer. Simulat.*, 32:63–80, 2016.

[9] M. Krüger, M. Groß, and P. Betsch. An energy-entropy-consistent time stepping scheme for nonlinear thermo-viscoelastic continua. *ZAMM*, 96(2):141–178, 2016.

[10] S. Conde Martín. *Energy-Entropy-Momentum Time Integration Methods for Coupled Smooth Dissipative Problems*. PhD Dissertation, Universidad Politécnica de Madrid, 2016.

[11] S. Conde Martín and J.C. García Orden. On Energy-Entropy-Momentum integration methods for discrete thermo-visco-elastodynamics. *Computers & Structures*, 181:3–20, 2017.

[12] P. Betsch, editor. *Structure-preserving Integrators in Nonlinear Structural Dynamics and Flexible Multibody Dynamics*, volume 565 of *CISM Courses and Lectures*. Springer-Verlag, 2016.

[13] P. Betsch and M. Schiebl. GENERIC-based formulation and discretization of initial boundary value problems for finite strain thermoelasticity. Submitted for publication in Comput. Methods Appl. Mech. Engrg., March 09, 2018.

[14] H.C. Öttinger. Nonequilibrium thermodynamics for open systems. *Physical Review E*, 73(3):036126–1–10, 2006.

[15] P. Betsch and M. Schiebl. Variational formulations for large strain thermo-elastodynamics based on the GENERIC formalism. In *Proceedings of the 6th European Conference on Computational Mechanics*, Glasgow, UK, 11-15 June 2018.

[16] Oscar Gonzalez. Time integration and discrete hamiltonian systems. *Journal of Nonlinear Science*, 6(5):449, 1996.